

# Parts-Per-Billion Carbon Monoxide Sensing in Silicon-on-Sapphire Mid-Infrared Photonic Crystal Waveguides

Ali Rostamian<sup>1</sup>, Joel Guo<sup>1</sup>, Swapnajit Chakravarty<sup>2</sup>, Chi-Jui Chung<sup>1</sup>, Duy Nguyen<sup>2</sup>, Ray T. Chen<sup>1,2</sup>

<sup>1</sup>Department of Electrical and Computer Engineering, University of Texas at Austin, 10100 Burnet Rd. Austin, TX 78758, USA

<sup>2</sup>Omega Optics, Inc., 8500 Shoal Creek Blvd., Bldg. 4, Suite 200, Austin, Texas 78757, USA

Author e-mail address: [ali.rostamian@utexas.edu](mailto:ali.rostamian@utexas.edu), [swapnajit.chakravarty@omegaoptics.com](mailto:swapnajit.chakravarty@omegaoptics.com), [chenrt@austin.utexas.edu](mailto:chenrt@austin.utexas.edu)

**Abstract:** We experimentally detect 3 ppm carbon monoxide via optical absorbance in a 1mm long slotted photonic crystal waveguide in silicon-on-sapphire at wavelength  $\lambda=4.55\mu\text{m}$ . Feasibility of low ppb sensing will be shown by design modifications. © 2018 The Author(s)

Infrared spectroscopy is widely accepted as a reliable and low cost technique in sensing applications. Owing to unique spectral signatures, it is possible to identify gases and vapors of interest with high sensitivity using this technique in variety of military, healthcare and environmental sensing applications. We previously demonstrated experimentally that various analytes in both liquid and gas phase can be detected to low parts per million (ppm) and parts per billion (ppb) levels on a silicon chip using slow light enhanced absorption spectroscopy [1-3]. The molecular fingerprint regions in the mid-infrared at wavelengths  $\lambda>3\mu\text{m}$  offer the advantage of larger absorption cross-sections of the fundamental vibration signatures of most analyte gases and vapors, in contrast to overtone signatures for  $\lambda<3\mu\text{m}$  that further enhances the detection sensitivity. Silicon (with optical transparency till  $\lambda\sim 8\mu\text{m}$ ) has been proposed as the desired mid-infrared waveguiding platform. The requirement of a low-loss cladding has made silicon-on-sapphire (SoS) an ideal chip candidate for applications till  $\lambda=5\mu\text{m}$ , for potentially more robust architectures versus free-standing silicon membranes [4]. In this paper, we experimentally study holey photonic crystal waveguides (HPCWs) in silicon-on-sapphire at mid-infrared wavelength of  $4.55\mu\text{m}$  and employ this structure to detect 3ppm of carbon monoxide (CO). We show feasibility of low ppb sensing by design modifications.

Fig. 1(a) shows the dispersion diagram of a HPCW obtained by plane-wave expansion (PWE) simulations, for operation at  $\lambda=4.55\mu\text{m}$ . Figs. 1(b) and (c) show top view and oblique view SEMs of our fabricated HPCW where  $r=0.18a$  is the radius of the bulk air holes in the hexagonal lattice with lattice constant  $a=1\mu\text{m}$ ,  $h=0.9a$  is the thickness of the PC slab and  $r_{SH}=0.5r$  is the radius of the small holes in the center of the HPCW. Figs. 2(a) and (b) show electric field intensity enhancement in the circular slots at the center of the photonic crystal (PC) waveguide.

The principle of infrared absorption spectroscopy is based on the Beer-Lambert law. According to this technique, transmitted intensity  $I$  is given by:  $I=I_0 \exp(-\gamma\alpha L)$  .....(1) where  $I_0$  is the incident intensity,  $\alpha$  is the absorption coefficient of the medium,  $L$  is interaction length and  $\gamma$  is the medium-specific absorption factor determined by dispersion enhanced light-matter interaction. In conventional free-space systems,  $\gamma=1$ ; thus  $L$  must be large to achieve a suitable sensitivity of measured  $I/I_0$ .

For lab-on-chip systems,  $L$  must be small, hence  $\gamma$  must be large. Mortensen et al showed [5] using perturbation

theory that  $\gamma = f \times \frac{c/n}{v_g}$  .....(2) where  $c$  is the velocity of light in free space,  $v_g$  is the group

velocity in medium of effective index  $n$  and  $f$  is the filling factor denoting relative fraction of optical field residing in the analyte medium. Eq. 2 shows that slow light propagation (small  $v_g$  or larger group index  $n_g$ ) significantly enhances absorption. Furthermore, greater the electric field overlap with analyte, greater the effective absorption by the medium. Both conditions of small  $v_g$  and high  $f$  are fulfilled in a slotted photonic crystal waveguide [1-3].

Device processing steps have been described in our previous SoS devices operating at  $\lambda=3.4\mu\text{m}$  [3, 6-8]. Processing conditions were optimized to etch a thicker  $h=900\text{nm}$  silicon slab for good out-of-plane optical confinement for operation at  $\lambda=4.55\mu\text{m}$ . Prior to sensing, the propagation characteristics of strip waveguides and slotted photonic crystal waveguides in SoS were characterized at  $\lambda=4.55\mu\text{m}$ . Light from a quantum cascade laser (QCL) was coupled into input strip waveguides from an optical fiber via grating couplers optimized for maximized coupling of transverse-electric (TE) polarized light required for propagation through slotted PCWs that only transmit TE-polarized light. Grating couplers at the output coupled light out of the waveguide to an external photodetector via an output optical fiber. Details of the measurement setup have been described in Ref. [3]. The propagation loss in the strip waveguides and slotted PCWs is 2dB/cm and 15dB/cm respectively as shown in Fig. 3. Although PCWs are best characterized by broadband / tunable sources covering the PCW transmission spectra, we have previously

demonstrated that the slow light guided mode wavelength bandwidth, the stop band width and propagation characteristics above the light line in photonic crystal waveguides, can be demonstrated experimentally using a single wavelength laser by varying the lattice constant ( $a$ ) of the device over several devices [3, 6]. We used the same method to determine the operating point in the dispersion diagram in Fig. 1(b) for our sensing experiments. Transmission was zero in the stopgap, while high transmission was observed for short 100 $\mu$ m long waveguides above the sapphire light line. As the waveguide became longer  $\sim$ 1mm, transmission above the light line decreased dramatically due to radiation loss. At 15dB/cm propagation loss, the total loss in a 1mm long holey photonic crystal waveguide was only 1.5dB.

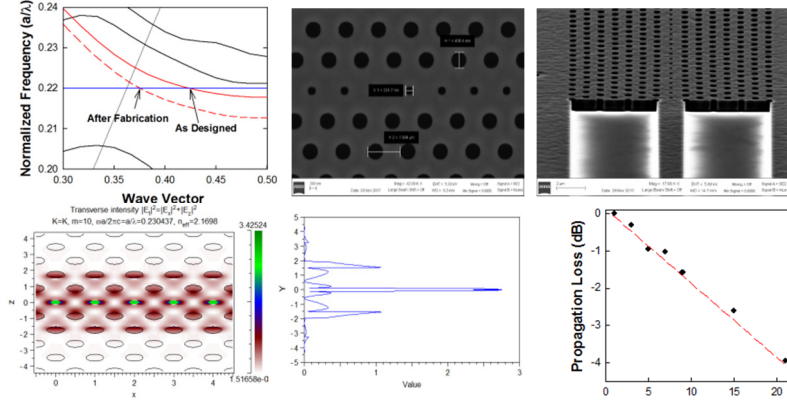


Fig. 1: PWE simulation showing the normalized frequency and operating point of slow light HPCW guided mode in the dispersion diagram. The new operating point of the device after fabrication is indicated for  $a=1000$ nm. SEMs showing top view and oblique view of the strip-waveguide-HPCW interface shown in (b) and (c) respectively.

Fig. 2: (a) Electric field intensity profile of the propagating slow light slotted photonic crystal waveguide mode at transmission band edge. (b) Transverse cross-section of electric field intensity in (a).

Fig. 3: (a) Propagation loss characteristics of strip waveguide in SoS at  $\lambda=4.55\mu$ m (b) Measurements showing the propagation loss characteristics of HPCW guided mode, at different lattice constant.

Fig. 4(a) shows the results of detection. At  $t=0$ , carrier nitrogen ( $N_2$ ) gas flows over the chip. At  $t=75$  seconds, when the CO gas is turned on, a 14% drop is observed in the measured signal. When CO is turned off at  $t=175$  seconds, with nitrogen carrier still flowing, the signal goes back to  $t=0$  levels. Measurements were done at 3ppm calibrated CO generation. Once released from the tubing, the gas spreads into the ambient before it reaches the chip. A ANSYS computational fluid dynamics simulation (Fig. 4(b)) of the experimental setup wherein the gas was ejected at 10-degree to the normal (with 531sccm carrier  $N_2$  flow), at a height of 2mm from the surface of the chip, indicates that the effective gas concentration at the chip surface, being detected by our 1mm long HPCW is also 3 ppm. The slopes observed in Fig. 4(a), during CO Turn-ON and Turn-OFF are symmetric and related to the flow rate of the carrier  $N_2$  which not only determines the effective concentration of CO but also the time it takes for the gas to flow from our calibrated Kintek vapor generator to the chip surface via the tubing.

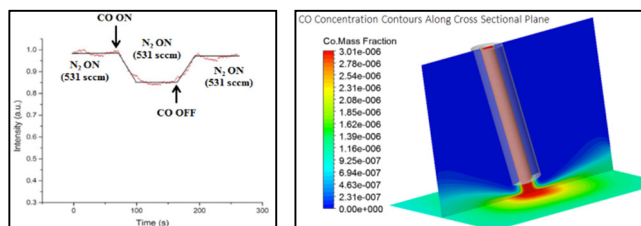


Fig. 4: (a) Experimental measurements of the lock-in amplifier signal versus time for CO switched ON and OFF, in constant flow carrier  $N_2$  gas (b) CFD simulations showing the effective gas concentrations at the slotted PCW surface. A 2cm $\times$ 2cm surface area representative of the SoS chip dimensions is simulated. Tube is 2mm from chip surface.

From simulations and experimental results, we estimated that  $f\sim 3$  and group index  $n_g\sim 8$  in the fabricated structures. A 6 $\times$  enhancement in sensitivity is anticipated by simply increasing the HPCW length to 6mm. By changing the wavelength interrogated from  $\lambda=4.55\mu$ m to  $\lambda=4.6\mu$ m, a 2 $\times$  enhancement in sensitivity is expected due to the intrinsic 2 $\times$  larger absorption cross-section of CO. A conservative  $n_g\sim 24$ , easily achieved in PCWs would result in a total (6 $\times$ 2 $\times$ 3=24) times enhancement that will allow sensing of (3/24) ppm =125ppb CO. Results will be demonstrated along with advanced designs to achieve sub-100ppb sensitivity. The research was supported by NASA SBIR Contract #NNX17CA44P and NSF Grant # 1711824.

**References**

[1] W-C. Lai, et al., Optics Lett. 36 (6), 984 (2011).  
 [2] W-C. Lai, et al., Appl. Phys. Lett. 98 (2), 023304 (2011)  
 [3] Y. Zou et al., Sens. and Actuators B: Chemical 221, 1094 (2015)  
 [4] R. Soref, Nat. Photon. 4(8), 495 (2010)  
 [5] N.A. Mortensen, et al., Appl. Phys. Lett. 90 (14), 141108 (2007)  
 [6] Y. Zou, et al., Opt. Express 23, 6965 (2015)  
 [7] Y. Zou et al., Appl. Phys. Lett., 107, 081109 (2015).  
 [8] Y. Zou et al., Appl. Phys. Lett.104, 141103 (2014)